

# Effects of the size of cosmological N-Body simulations on physical quantities — I: Mass Function

J. S. Bagla<sup>1</sup> and Jayanti Prasad<sup>2</sup>

<sup>1, 2</sup> Harish-Chandra Research Institute, Chhatnag Road, Jhusi, Allahabad 211019, India.

E-mail: <sup>1</sup> jasjeet@hri.res.in, <sup>2</sup> jayanti@hri.res.in

2 December 2024

## ABSTRACT

N-Body simulations are a very important tool in the study of formation of large scale structures. Much of the progress in understanding the physics of high redshift universe and comparison with observations would not have been possible without N-Body simulations. Given the importance of this tool, it is essential to understand its limitations as ignoring the limitations can easily lead to interesting but unreliable results. In this paper we study some of the limitations arising out of the finite size of simulation volume. We explicitly construct the correction term arising due to a finite box size and study its generic features for clustering of matter and also on mass functions. We show that the correction to mass function is maximum near the scale of non-linearity, as a corollary we show that the correction term to the multiplicity function and the number density of haloes of a given mass changes sign at this scale; the number of haloes at small masses is over estimated in simulations. The same technique can be used to study corrections on other physical quantities. We point out situations in which a box that is much larger than the scale of non-linearity is used and even then the correction term is comparable to the physical quantity of interest.

**Key words:** methods: N-Body simulations, numerical – gravitation – cosmology : theory, dark matter, large scale structure of the universe

## 1 INTRODUCTION

Large scale structures like galaxies and clusters of galaxies are believed to have formed by gravitational amplification of small perturbations (Peebles 1980; Peacock 1999; Padmanabhan 2002; Bernardeau et al. 2002). Observations suggest that the initial density perturbations were present at all scales that have been probed by observations. An essential part of the study of formation of galaxies and other large scale structures is thus the evolution of density perturbations for such initial conditions. The basic equations for this have been known for a long time (Peebles 1974) and these equations are easy to solve when the amplitude of perturbations is small. Once the amplitude of perturbations at relevant scales becomes large, i.e.,  $\delta \sim 1$ , the perturbation becomes non-linear and the coupling with perturbations at other scales cannot be ignored. The equation for evolution of density perturbations cannot be solved for generic perturbations in the non-linear regime. N-Body simulations (Bertschinger 1998; Bagla 2005) are often used to study the evolution in this regime, unless one requires only a limited amount of information and quasi-linear approximation schemes (Zel'dovich 1970; , 1989; Matarrese et al. 1992; Brainerd et al. 1993; Bagla & Padmanabhan 1994; Sahni & Coles 1995; Hui & Bertschinger 1996; Bernardeau et al. 2002) or scaling relations (Davis & Peebles 1977; Hamilton et al. 1991; Jain et al. 1995; Kanekar 2000; Ma 1998; Nityananda & Padmanabhan 1994;

Padmanabhan et al. 1996; Peacock & Dodds 1994; Padmanabhan 1996; Peacock & Dodds 1996; Smith et al. 2003) suffice.

In N-Body simulations, we simulate a representative region of the universe. This representative region is a large but finite volume and periodic boundary conditions are often used – a convenient choice considering that the universe does not have a boundary. Typically the simulation volume is taken to be a cube. Effect of perturbations at scales smaller than the mass resolution of the simulation, and of perturbations at scales larger than the box is ignored. Indeed, even perturbations at scales comparable to the box are under sampled.

It has been shown that for gravitational dynamics in an expanding universe, perturbations at small scales do not influence collapse of large scale perturbations in a significant manner (Peebles 1974, 1985; Little et al. 1991; Bagla & Padmanabhan 1997; Couchman & Peebles 1998) as far as the correlation function or power spectrum at large scales are concerned. Therefore we may assume that ignoring perturbations at scales much smaller than the scales of interest does not affect results of N-Body simulations. However, there may be other effects that are not completely understood at the quantitative level (Bagla, Prasad & Ray 2005) even though these have been seen only in somewhat artificial situations.

Perturbations at scales much larger than the simulation volume can affect the results of N-Body simulations. Use of periodic boundary conditions implies that the average density in the simu-

## 2 Bagla and Prasad

lation box is same as the average density in the universe, in other words we are assuming that there are no perturbations at the scale of the simulation volume (or at larger scales). Therefore the size of the simulation volume should be chosen so that the amplitude of fluctuations at that scale (and at larger scales) is ignorable. If the amplitude of perturbations at larger scales is not ignorable and the simulations do not take the contribution of these scales into account then clearly the simulation will not be a faithful representation of the model being simulated. It is not obvious as to when fluctuations at larger scales can be considered ignorable, indeed the answer to this question will depend on the physical quantity of interest as well as the model being studied.

If the amplitude of density perturbations at the box scale is small but not ignorable, simulations underestimate the correlation function though the number density of small mass haloes does not change by much (Gelb & Bertschinger 1994a,b). In other words, the formation of small haloes is not disturbed but their distribution is affected by non-inclusion of long wave modes. The mass function of massive haloes changes significantly (Gelb & Bertschinger 1994a,b). The void spectrum is also affected by finite size of the simulation volume if perturbations at large scales are not ignorable (Kauffmann & Melott 1992). It has been shown that properties of a given halo can change significantly as the box size changes but the distribution of most properties remains unchanged (Power & Knebe 2005).

Significance of perturbations at large scales has been discussed in detail and a method (MAP) has been devised for incorporating the effects of these perturbations (Tormen & Bertschinger 1996). These methods make use of the fact that if the box size is chosen to be large enough then the contribution of larger scales can be incorporated by adding displacements due to the larger scales independently of the evolution of the system in an N-Body simulation. The motivation for development of such a tool is to enhance the range of scales over which results of an N-Body simulation can be used by improving the description at scales comparable to the box size. Such an approach ignores the coupling of large scale modes with small scale modes and this again brings up the issue of what is a large enough scale for a given model such that these methods can be used without introducing errors. Large scales contribute to displacements and velocities, and variations in density due to these scales modify the rate of growth for small scales perturbations (Cole 1997).

In some cases, one may be able to devise a method to ‘‘correct’’ for the effects of a finite box-size (Colombi et al. 1994), but such methods cannot be generalised to other statistical measures.

Effects of a finite box size modify values of physical quantities even at scales much smaller than the simulation volume (Bagla & Ray 2005) (BR05, hereafter). In BR05, we suggested use of the fraction of mass in collapsed haloes as an indicator of the effect of a finite box size. We showed that unless the simulation volume is large enough, the fraction of mass in collapsed haloes will be underestimated and as the collapsed fraction is less sensitive to box-size we can expect several other statistical indicators of clustering to deviate significantly from expected values in such simulations. A workaround for this problem was suggested in the form of an ensemble of simulations to take the effect of convergence due to long wave modes into account (Sirk 2005), the effects of shear are not taken into account in this approach. Another study showed that the distribution of most internal properties of haloes, e.g., concentration, triaxiality and angular momentum do not change considerably with the box size even though properties of a given halo may change considerably (Power & Knebe 2005). In this paper we

generalise the approach suggested in BR05 and write down an explicit correction term for a number of statistical indicators of clustering. This allows us to study generic properties of the expected correction term in any given case, apart of course from allowing us to evaluate the magnitude of the correction as compared to the expected value of the given statistical indicator. We apply this technique to mass functions in this paper.

## 2 BASIC EQUATIONS

Initial conditions for N-Body simulations are often taken to be a realisation of a Gaussian random field with a given power spectrum. The power spectrum is sampled at discrete points in the  $\mathbf{k}$  space between the scales corresponding to the box size (fundamental mode) and the grid size (Nyquist frequency mode). Sampling of the power spectrum is dense towards the Nyquist mode, but is sparse as we get closer to the fundamental mode. Power spectra for density, potential and the velocity field are related to each other in the linear regime. These can be used to compute the second moment, either two point functions or *rms* fluctuations. These can be expressed as a sum over power spectrum at these points, weighted by an appropriate window function. In the peak picture, most quantities of interest can be related to the second moment or the two point correlation function (Bardeen et al. 1986), therefore a method for estimating box-size correction in the second moment can be used as a base for computing correction for other physical quantities.

### 2.1 Clustering Amplitude

We now present our approach for estimating the effects of a finite box size on physical quantities in the linear limit. We will illustrate our approach using *rms* fluctuations in mass  $\sigma(r)$ , but it can be generalised to any other quantity in a straightforward manner.

$$\begin{aligned}
\sigma^2(r, L_{\text{box}}) &\simeq \frac{9}{V} \sum_{\mathbf{k}} P(k) \left[ \frac{\sin kr - kr \cos kr}{k^3 r^3} \right]^2 \\
&\simeq \int_{2\pi/L_{\text{box}}}^{2\pi/L_{\text{grid}}} \frac{dk}{k} \frac{k^3 P(k)}{2\pi^2} 9 \left[ \frac{\sin kr - kr \cos kr}{k^3 r^3} \right]^2 \\
&\simeq \int_{2\pi/L_{\text{box}}}^{\infty} \frac{dk}{k} \frac{k^3 P(k)}{2\pi^2} 9 \left[ \frac{\sin kr - kr \cos kr}{k^3 r^3} \right]^2 \\
&= \int_0^{\infty} \frac{dk}{k} \frac{k^3 P(k)}{2\pi^2} 9 \left[ \frac{\sin kr - kr \cos kr}{k^3 r^3} \right]^2 \\
&\quad - \int_0^{2\pi/L_{\text{box}}} \frac{dk}{k} \frac{k^3 P(k)}{2\pi^2} 9 \left[ \frac{\sin kr - kr \cos kr}{k^3 r^3} \right]^2 \\
&= \sigma_0^2(r) - \sigma_1^2(r, L_{\text{box}})
\end{aligned} \tag{1}$$

Here  $P(k)$  is the power spectrum of density contrast,  $\sigma_0^2(r)$  is the expected level of fluctuations in mass at scale  $r$  for the given power spectrum and  $\sigma^2(r, L_{\text{box}})$  is what we get in an N-Body simulation at early times. We have assumed that we can approximate the sum over the  $k$  modes sampled in initial conditions by an integral. Further, we make use of the fact that small scales do not influence large scales to ignore the error contributed by the upper limit of the in-

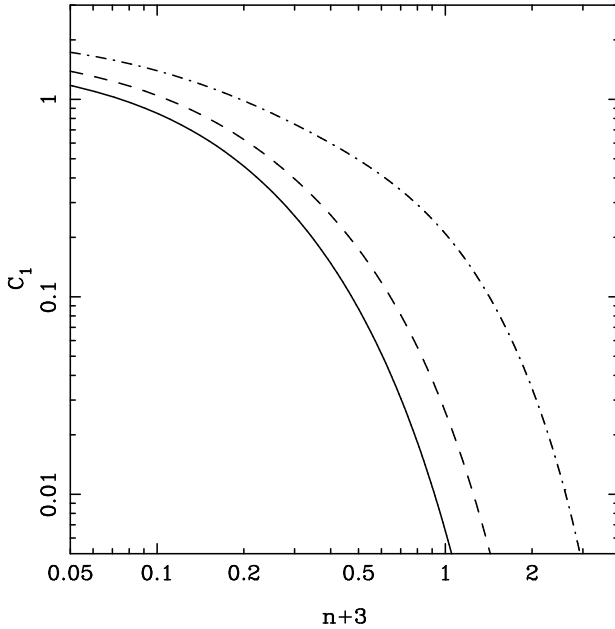


**Figure 1.** This figure shows the first correction term  $C_1$  (see Eqn.(4)) for power law models with index  $n$  normalised such that  $\sigma_0^2(r_{nl}) = 1$ . The curves here are for  $L_{\text{box}}/r_{nl} = 16$  (dot-dashed curve),  $L_{\text{box}}/r_{nl} = 128$  (dashed curve) and  $L_{\text{box}}/r_{nl} = 512$  (solid curve).  $C_1$  is plotted as a function of  $n + 3$  and we find that the correction term increases as  $n + 3 \rightarrow 0$ . See text for more details.

tegral. This approximation is valid as long as the scales of interest are more than a few grid lengths.

In the approach outlined above, the value of  $\sigma^2$  at a given scale is expressed as a combination of the expected value  $\sigma_0^2$  and the correction due to the finite box size  $\sigma_1^2$ . Here  $\sigma_0^2$  is independent of the box size and depends only on the power spectrum and scale of interest. It is clear that  $\sigma^2(r, L_{\text{box}}) \leq \sigma_0^2(r)$  and also  $\sigma_1^2(r, L_{\text{box}}) \geq 0$ . It can also be shown that for hierarchical models,  $d\sigma_1^2(r, L_{\text{box}})/dr \leq 0$ , i.e.,  $\sigma_1^2(r, L_{\text{box}})$  increases or saturates to a constant value as we approach small  $r$ .

If the scale of interest is much smaller than the box-size  $L_{\text{box}}$  then,

$$\begin{aligned}
 \sigma_1^2(r, L_{\text{box}}) &= \int_0^{2\pi/L_{\text{box}}} \frac{dk}{k} \frac{k^3 P(k)}{2\pi^2} 9 \left[ \frac{\sin kr - kr \cos kr}{k^3 r^3} \right]^2 \\
 &\approx \int_0^{2\pi/L_{\text{box}}} \frac{dk}{k} \frac{k^3 P(k)}{2\pi^2} \\
 &\quad - \frac{r^2}{5} \int_0^{2\pi/L_{\text{box}}} \frac{dk}{k} \frac{k^5 P(k)}{2\pi^2} \\
 &\quad + \frac{3r^4}{175} \int_0^{2\pi/L_{\text{box}}} \frac{dk}{k} \frac{k^7 P(k)}{2\pi^2} + \mathcal{O}(r^6) \quad (2) \\
 &= C_1 - C_2 r^2 + C_3 r^4 + \mathcal{O}(r^6) \quad (3)
 \end{aligned}$$

The small parameter in the expansion is  $r/L_{\text{box}}$ . This expansion is useful if  $k^3 P(k)$  goes to zero as we approach  $k = 0$ . It is interesting to note that the first term is scale independent. The numerical values of  $C_i$  can be used to estimate the scale below which  $\sigma_1$  can

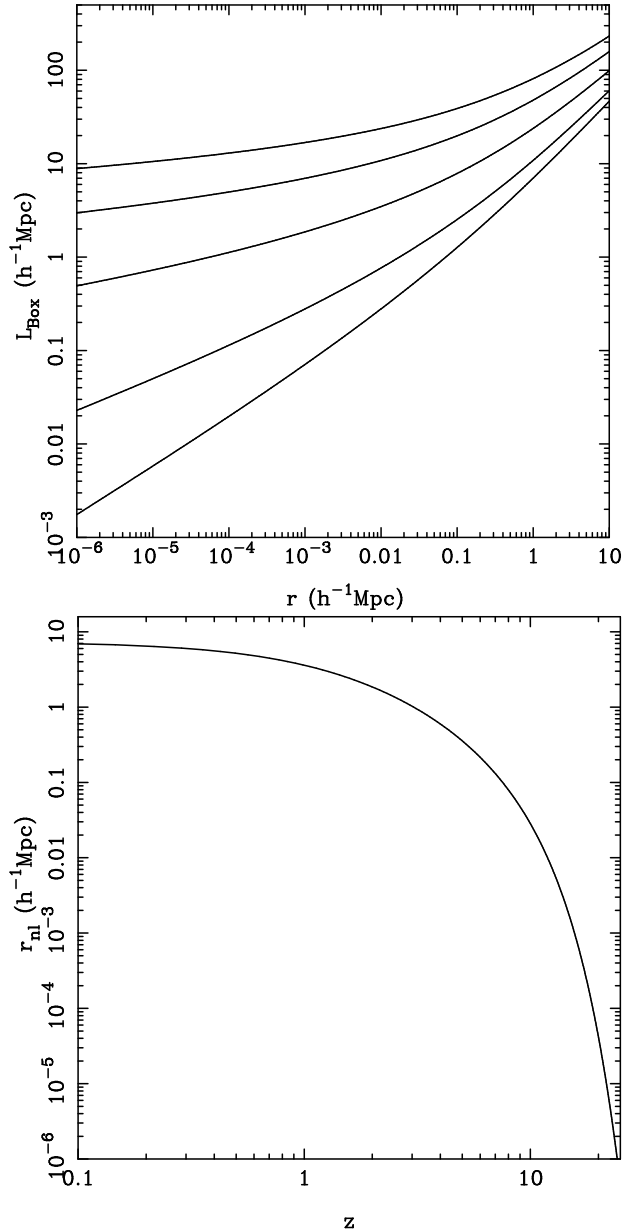


**Figure 2.** The top panel shows curves of constant  $C_1(L_{\text{box}})/\sigma_0^2(r)$  on the  $r - L_{\text{box}}$  plane for the  $\Lambda$ CDM model (see text for details). Lines mark  $C_1/\sigma_0^2 = 0.01, 0.03, 0.1, 0.3$  and  $0.5$ , from top to bottom. The lower panel shows the scale of non-linearity  $r_{nl}$  as a function of redshift for the  $\Lambda$ CDM model.

be approximated by a constant. Later terms have a scale dependence and the noteworthy feature is that modes closer to  $2\pi/L_{\text{box}}$  contribute most significantly to the integral.

It is noteworthy that the first term,  $C_1$ , has the same value for all choices of window functions that approach unity at small  $k$ . By virtue of this fact,  $C_1$  is also the correction for the two point correlation function  $\xi(r)$  at sufficiently small scales.

At large scales  $\sigma_0^2(r)$  and  $\sigma_1^2(r, L_{\text{box}})$  have a similar magnitude and the *rms* fluctuations in the simulation become negligible compared to its expected value in the model. As we approach small  $r$  the error term  $\sigma_1^2(r, L_{\text{box}})$  is constant and for most models it becomes insignificant in comparison with  $\sigma_0^2(r)$  if the expected *rms* fluctuations keep on increasing. In models where  $\sigma_0^2(r)$  increases

**Table 1.** This table lists corrections due to a finite box-size to indicators of clustering in the limit  $r \ll L_{\text{box}}$ . These expressions are equivalent to Eqn.(3) and constants  $C_i$  are the same as in that equation.

Indicator	Correction
$\xi(r)$	$C_1 - \frac{5}{6}C_2r^2 + \frac{35}{72}C_3r^4 + \mathcal{O}(r^6)$
$\bar{\xi}(r)$	$C_1 - \frac{1}{2}C_2r^2 + \frac{5}{24}C_3r^4 + \mathcal{O}(r^6)$

very slowly at small scales or saturates to a constant value, we can have a situation where the correction term  $\sigma_1^2$  is significant at all scales. To illustrate this point, we give the expression for  $C_1$  for power law models with  $P(k) = Ak^n$ :

$$C_1 = \frac{1}{n+3} \frac{A}{2\pi^2} \left( \frac{2\pi}{L_{\text{box}}} \right)^{n+3} \quad (4)$$

Clearly, this becomes more and more significant as  $n \rightarrow -3$ . We illustrate this in Figure 1 where we have plotted  $C_1$  as a function of  $n+3$ . We fix  $A$  by choosing a scale of non-linearity  $r_{nl}$  such that  $\sigma_0(r_{nl}) = 1$ . Curves are plotted for three values of  $L_{\text{box}}/r_{nl}$ :  $L_{\text{box}}/r_{nl} = 16$  (dot-dashed curve),  $L_{\text{box}}/r_{nl} = 128$  (dashed curve) and  $L_{\text{box}}/r_{nl} = 512$  (solid curve). As  $\sigma_0$  is unity at the scale of non-linearity and  $C_1$  is the first order correction, clearly we require  $C_1 \ll 1$  for the error due to box size to be small and hence ignorable. If we fix  $C_1 \leq 0.1$  then we can simulate  $n = -1$  with  $L_{\text{box}}/r_{nl} = 16$  but for more negative indices we require a larger separation between the box size and the scale of non-linearity. We can just about manage  $n = -2.3$  with  $L_{\text{box}}/r_{nl} = 128$  with the same threshold on error, and with  $L_{\text{box}}/r_{nl} = 512$  we can go up to  $n = -2.5$ . As N-Body simulations are most useful for studying non-linear evolution, even the largest simulations possible today will be left with a small range of scales over which  $\sigma_0 \geq 1$ . This outlines the pitfalls of trying to simulate models with  $n \simeq -3$  at the entire range of scales.

The same applies if the power spectrum of interest has  $n \simeq -3$  at all scales of interest. Figure 2 (top panel) shows lines of constant  $C_1/\sigma_0^2$  in the  $L_{\text{box}} - r$  plane for the  $\Lambda$ CDM. We chose  $n = 1$ ,  $h = 0.7$ ,  $\Omega_\Lambda = 0.3$ ,  $\Omega_{nr} = 0.3$  and  $\sigma_8 = 0.9$ . We ignored the effects of Baryons on the power spectrum. From top to bottom, the lines correspond to  $C_1/\sigma_0^2 = 0.01, 0.03, 0.1, 0.3$  and  $0.5$ . It is noteworthy that a box-size of smaller than 0.5Mpc is precluded if we insist on  $C_1(L_{\text{box}})/\sigma_0^2(r) \leq 0.1$ , irrespective of the scale of interest. This implies that we cannot expect to simulate scales smaller than about 500 pc without considerable improvement in the dynamic range of cosmological N-Body simulations. As we are using the linearly evolved quantities for our argument, the comments on box size are valid irrespective of the redshift up to which the simulation is run. The contours do not change if we use  $\sigma_1^2$  instead of  $C_1$ .

The lower panel of the same figure shows the scale of non-linearity for the same  $\Lambda$ CDM model as a function of redshift.

For reference, we have given expressions equivalent to Eqn.(3) for the correction to  $\xi$  and  $\bar{\xi}$  in Table 1.

## 2.2 Velocities

We can use the method outlined above to estimate correction to the velocity field. Velocities and density contrast are related to one another (Peebles 1980) in the linear regime. The power spectra for these two are related as  $P_v(k) \propto P(k)/k^2$ . Thus velocities at any

given scale depend more strongly on the power spectrum at large scales (small  $k$ ) than density fluctuations. This implies that the correction term will be more significant for velocities than what we have computed above using the clustering amplitude at scales of interest. We will discuss the corrections in velocity field in detail in a follow up paper.

## 2.3 Mass Function

We can use the explicit correction for *rms* fluctuations ( $\sigma$ ) to estimate a similar correction for mass functions of haloes. We shall use Press-Schechter approach (Press & Schechter 1974; Bond et al. 1991) to begin with, but we will also give results for the Sheth-Tormen mass function (Sheth & Tormen 1999; Sheth, Mo, & Tormen 2001) to demonstrate that our results are generic in nature.

The mass fraction in collapsed haloes with mass greater than  $M$  in the Press-Schechter model is given by

$$F(M, L_{\text{box}}) = \text{erfc} \left( \frac{\delta_c}{\sigma(M, L_{\text{box}})\sqrt{2}} \right) = \frac{2}{\sqrt{\pi}} \int_{\delta_c/\sigma(M, L_{\text{box}})\sqrt{2}}^{\infty} \exp[-x^2] dx \quad (5)$$

Where  $\delta_c$  ( $\simeq 1.68$ ) is a parameter<sup>1</sup> and  $M$  is related to the scale  $r$  through the usual relation. We can write  $F$  as the contribution expected in the limit  $L_{\text{box}} \rightarrow \infty$  and a correction due to the finite box size.

$$F(M, L_{\text{box}}) = \frac{2}{\sqrt{\pi}} \int_{\delta_c/\sigma_0(M)\sqrt{2}}^{\infty} \exp[-x^2] dx - \frac{2}{\sqrt{\pi}} \int_{\delta_c/\sigma_0(M)\sqrt{2}}^{\delta_c/\sigma(M, L_{\text{box}})\sqrt{2}} \exp[-x^2] dx = F_0(M) - F_1(M, L_{\text{box}}) \quad (6)$$

The correction to  $F(M)$  due to the finite box size always leads to an under-estimate as  $F_1(M, L_{\text{box}})$  is always positive. This is consistent with what we found in BR05. However,  $F_1(M, L_{\text{box}})$  is not a monotonic function of  $M$  as it goes to zero at small as well as large  $M$ . At small  $M$  ( $M \ll M_{nl}$ )<sup>2</sup>, the limits of the integral differ by a very small amount. This difference ( $\delta_c\sigma_1^2/2\sqrt{2}\sigma_0^3$ ) keeps on decreasing as we get to small  $M$  while the integrand remains finite. Therefore we expect  $F_1$  to decrease at small  $M$ . At these scales, we can write an approximate expression for  $F_1(M)$ :

$$F_1(M) \simeq \frac{\delta_c}{\sqrt{2\pi}} \frac{\sigma_1^2}{\sigma_0^3} \exp \left[ -\frac{\delta_c^2}{2\sigma_0^2} \right] . \quad (7)$$

This clearly decreases as we go to small  $M$ :  $\sigma_1$  goes over to the constant  $C_1$  and  $\sigma_0$  keeps increasing.

At large  $M$  ( $M \gg M_{nl}$ ), both  $\sigma(M, L_{\text{box}})$  and  $\sigma_0(M)$  are small and the limits of the integral cover the region where the integrand is very small. Thus we expect  $F_1(M, L_{\text{box}})$  to become smaller as we go to larger  $M$  in this regime. At these scales, we

<sup>1</sup> In the spherical collapse model, this is the linearly extrapolated density contrast at which we expect the halo to virialise Gunn & Gott (1972).

<sup>2</sup>  $M_{nl}$  is the mass corresponding to the scale where  $\sigma_0 = 1$  and we shall assume that  $L_{\text{box}}$  is much larger than this scale.

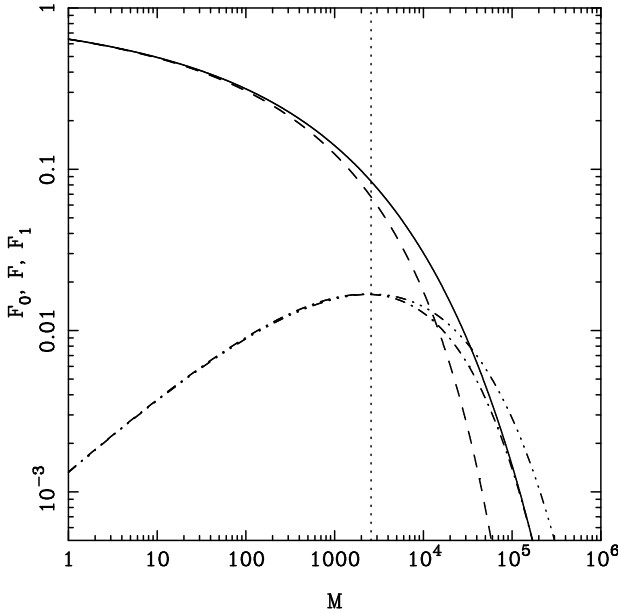


**Figure 3.** The Press-Schechter mass function and correction terms are plotted as a function of mass.  $F_0(M)$  (solid curve),  $F(M)$  (dashed curve) and  $F_1(M)$  (dot-dashed curve) are shown here. The scale where  $\sigma_0 = \delta_c/\sqrt{3}$  is marked with a vertical dotted line, we see that this estimate coincides with the maximum of  $F_1(M)$ . The correction term  $F_1(M)$  is more than 10% of  $F_0(M)$  at this scale. Also shown is the approximate expression Eqn.(7) for  $F_1(M)$  (dot-dot-dot-dashed curve) and we note that it follows the actual curve to masses greater than  $M_{nl}$ .

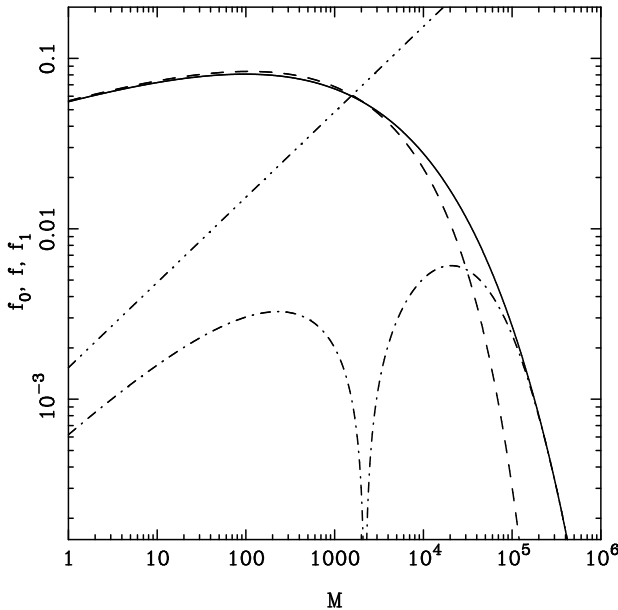


**Figure 4.** The Press-Schechter multiplicity function and correction terms are plotted as a function of mass.  $f_0(M)$  (solid curve),  $f(M)$  (dashed curve) and  $f_1(M)$  (dot-dashed curve) are shown here. The scale where  $\sigma_0 = \delta_c/\sqrt{3}$  is marked with a vertical dotted line, we see that this estimate coincides with change of sign for  $f_1(M)$ . At scales below this, the correction term  $f_1(M)$  is positive and hence there are more haloes in simulation than expected in the model. Also shown is the approximate expression for  $f_1(M)$  (dot-dot-dot-dashed curve).

also expect  $F_0$  and  $F_1$  to become almost equal while  $F(M)$  goes to zero faster than either term. Therefore  $F_1(M, L_{\text{box}})$  must have a maxima at an intermediate scale. The scale at which the maxima occurs can be found by solving the following equation.

$$\begin{aligned} \frac{d \log \sigma_1^2}{d \log \sigma_0^2} &= -\frac{\sigma_0^2}{\sigma_1^2} \left[ \frac{\sigma}{\sigma_0} \left( 1 - \frac{\sigma_1^2}{\sigma_0^2} \right) \exp \left[ \frac{\delta_c^2 \sigma_1^2}{2 \sigma^2 \sigma_0^2} \right] - 1 \right] \\ &\simeq \frac{3}{2} - \frac{\delta_c^2}{2 \sigma_0^2} \end{aligned} \quad (8)$$

Here, the second equation is obtained if  $\sigma_1 \ll \sigma_0$ . If  $L_{\text{box}} \gg r_{nl}$ , where  $r_{nl}$  is the scale of non-linearity then  $\sigma_1$  is very well approximated by the Taylor series Eqn.(3) around this scale and  $\sigma_1$  is a very slowly varying function of scale. Thus  $F_1(M, L_{\text{box}})$  has a maxima at  $\sigma_0 = \delta_c^2/3 \sim 1$  if the first term in Eqn.(3) is a good approximation for  $\sigma_1$ . If scale dependent terms in Eqn.(3) are not ignorable then the maxima of  $F_1(M, L_{\text{box}})$  shifts to smaller scales in a manner that depends on the power spectrum and choice of box-size  $L_{\text{box}}$ .

Figure 3 shows the Press-Schechter mass function  $F(M)$  for a power law model with  $n = -2$ ,  $L_{\text{box}}/r_{nl} = 16$ . We have plotted  $F_0(M)$  (solid curve),  $F(M)$  (dashed curve) and  $F_1(M)$  (dot-dashed curve) as a function of  $M$ . The scale where  $\sigma_0 = \delta_c/\sqrt{3}$  is marked with a vertical dotted line, we see that this estimate coincides with the maximum of  $F_1(M)$ . The correction term  $F_1(M)$  is more than 10% of  $F_0(M)$  at this scale. Also shown is the approximate expression Eqn.(7) for  $F_1(M)$  (dot-dot-dot-dashed curve) and we note that it follows the actual curve to masses greater than  $M_{nl}$ . This figure illustrates all the generic features of corrections to mass function that we have discussed above.

The multiplicity function ( $f$ ) is defined as the fraction of mass in a logarithmic interval in mass:

$$\begin{aligned} f(M, L_{\text{box}}) d \log M &= -\frac{\partial F(M, L_{\text{box}})}{\partial \log M} d \log M \\ \Rightarrow f(M, L_{\text{box}}) &= -\frac{dF_0(M)}{d \log M} + \frac{\partial F_1(M, L_{\text{box}})}{\partial \log M} \\ &= f_0(M) - f_1(M, L_{\text{box}}). \end{aligned} \quad (9)$$

It is not possible to reduce this expression further while writing the correction term due to the finite box size separately. We can, however, ascertain generic properties of the correction term  $f_1(M, L_{\text{box}})$  from our understanding of  $F_1(M, L_{\text{box}})$ . At large  $M$ ,  $f_1$  is positive as  $F_1(M, L_{\text{box}})$  decreases with increasing  $M$ . Thus the mass fraction of haloes in this mass range is underestimated in simulations. We know that  $f_1$  has a zero near the scale of non-linearity as  $F_1$  has a maxima here. Thus there is a scale where corrections due to a finite box size vanish. At smaller scales, the slope of  $F_1$  and hence  $f_1$  changes sign and the correction to mass fraction in haloes is positive. A finite box size leads to an *over estimate* of number of low mass haloes. The magnitude of over estimate depends on  $\sigma_1$ , and hence on the slope of the power spectrum. In the limit of  $M \ll M_{nl}$ , we can use Eqn.(7) to compute the magnitude of over estimate:

$$f(M) \simeq f_0(M) + \frac{3\delta_c}{\sqrt{2\pi}} \frac{C_1}{\sigma_0^4} \left| \frac{d\sigma_0}{d \log M} \right|. \quad (10)$$

The correction term scales as  $M^{(n+3)/2}$  for power law models, i.e., it diverges as  $n \rightarrow -3$ . Clearly, the term will also be large for CDM like power spectra if the slope of the power spectrum around the box size is close to  $-3$ .

Figure 4 shows the Press-Schechter multiplicity function and correction terms are as a function of mass for the model used in

## 6 Bagla and Prasad

Figure 3. The expected multiplicity function  $f_0(M)$  (solid curve), what is expected in the simulation  $f(M)$  (dashed curve) and the correction term  $f_1(M)$  (dot-dashed curve) are shown here. The scale where  $\sigma_0 = \delta_c/\sqrt{3}$  is marked with a vertical dotted line, we see that this coincides with change of sign for  $f_1(M)$ . At scales below this, the correction term  $f_1(M)$  is positive and hence there are more haloes in simulation than expected in the model. Also shown is the approximate expression for  $f_1(M)$  (dot-dot-dot-dashed curve) in the limit  $M \ll M_{nl}$ . Unlike the approximation for  $F_1(M)$  which was accurate over a large range of scales, this is expected to be valid only in the limit of  $M \ll M_{nl}$  and indeed, is off by about a factor of two at the smallest scales shown here. However, it is a good approximation if we go to even smaller masses. We note that for this model, the over estimate of multiplicity function due to the finite box is small and therefore is difficult to detect. For this model,  $C_1/\sigma_0^2 \simeq 0.2$  at the scale of non-linearity and is smaller than 0.1 at scales where the over estimate in  $f(M)$  is maximum.

### 2.3.1 Sheth-Tormen Mass Function

We now give corresponding formulae for the Sheth-Tormen mass function (Sheth & Tormen 1999; Sheth, Mo, & Tormen 2001). The definition of mass function (Eqn.5) is modified to:

$$F(M, L_{\text{box}}) = \frac{2}{\sqrt{\pi}} \int_{\delta_c/\sigma(M, l_{\text{box}})\sqrt{2}}^{\infty} A(1+x^{-2q}) \exp[-x^2] dx \quad (11)$$

In the limit of  $A = 0.5$  and  $q = 0$  this is identical to the usual Press-Schechter mass function (Eqn.5). The maxima of the correction term ( $F_1(M, L_{\text{box}})$ ) occurs when the following equation is satisfied:

$$\begin{aligned} \frac{d \log \sigma_1^2}{d \log \sigma_0^2} &= -\frac{\sigma_0^2}{\sigma_1^2} \left[ \frac{\sigma}{\sigma_0} \left( 1 - \frac{\sigma_1^2}{\sigma_0^2} \right) \right. \\ &\quad \left. \exp \left[ \frac{\delta_c^2 \sigma_1^2}{2\sigma^2 \sigma_0^2} \right] \frac{1 + \left( \frac{\delta_c}{\sqrt{2}\sigma_0} \right)^{-2q}}{1 + \left( \frac{\delta_c}{\sqrt{2}\sigma} \right)^{-2q}} - 1 \right] \\ &\simeq \frac{3}{2} - \frac{\delta_c^2}{2\sigma_0^2} - q \left( \frac{\delta_c}{\sqrt{2}\sigma_0} \right)^{-2q} \end{aligned} \quad (12)$$

As before, this reduces to the expression in the Press-Schechter case (Eqn.8) in the limit  $q = 0$ . The qualitative features of the finite box correction to mass function are the same for the two prescriptions and may be considered to be generic. For reference, we write approximate expressions for correction to the mass function  $F(M)$ :

$$F_1 \simeq \frac{\delta_c}{\sqrt{2\pi}} \frac{\sigma_1^2}{\sigma_0^3} \exp \left[ -\frac{\delta_c^2}{2\sigma_0^2} \right] A \left[ 1 + \left( \frac{\delta_c}{\sqrt{2}\sigma_0} \right)^{-2q} \right] \quad (13)$$

and the multiplicity function  $f(M)$ :

$$f_1 = \frac{3\delta_c}{\sqrt{2\pi}} \frac{C_1}{\sigma_0^4} \left( \frac{d\sigma_0}{d \log M} \right) A \left[ 1 + \left( 1 - \frac{2q}{3} \right) \left( \frac{\delta_c}{\sqrt{2}\sigma_0} \right)^{-2q} \right] \quad (14)$$

for the Sheth-Tormen mass function.

## 3 DISCUSSION

In the preceeding section, we have described a method to estimate errors in the descriptors of clustering in the linear regime. We have shown that the error is typically small if the scale of interest is sufficiently smaller than the box size. An implicit requirement is that the scale of non-linearity too should be much smaller than the box size, if this restriction is overlooked then we will not only be ignoring power in modes larger than the simulation box but also the effects of mode coupling. Therefore, we require  $r, r_{nl} \ll L_{\text{box}}$ . Precisely how large  $L_{\text{box}}/r_{nl}$  should be depends on the power spectrum and this ratio is required to be very large as the slope of the power spectrum approaches  $-3$ . We used  $\sigma_1^2/\sigma_0^2$  as an indicator of the significance of the finite box size, any descriptor of second moment can be used but  $\sigma$  has the virtue of being positive definite at all scales. Our proposal is that  $\sigma_1^2(r)/\sigma_0^2(r), \sigma_1^2(r_{nl}(z))/\sigma_0^2(r_{nl}(z)) \ll 1$ , where all the  $\sigma$ s are evolved linearly. For power law models, corrections are significant for models with more large scale power. As a result of these corrections, the amplitude of density perturbations is not a power law and the range of scales over which it can be approximated by one becomes smaller as we approach  $n + 3 \rightarrow 0$ . In the linear regime, the radial pair velocity is related directly with  $\xi$  Peebles (1980); Nityananda & Padmanabhan (1994). As  $\xi$  is not a pure power law in simulations due to box-size corrections, we expect that the pair velocities will also deviate from expected values. This, in turn leads to deviations from scale invariant growth of density perturbations. This explains the difficulty in getting scale invariant evolution for models like  $n = -2$  in N-Body simulations Jain & Bertschinger (1996, 1998). For realistic models like the  $\Lambda$ CDM, the restrictions are stringent only if the scales of interest are below a few kpc and become even more stringent if we are interested in scales below a kpc (see Figure 2). Indeed, at these small scales we may require  $L_{\text{box}}/r \sim 10^4$  or even greater in order to manage  $C_1/\sigma_0^2 = 0.1$ . Of course, a bigger simulation volume is required if we demand better accuracy.

We showed that at sufficiently small scales the correction due to finite box size can be written as a series of progressively smaller terms. The first correction term ( $C_1$ ) is shown to be positive definite. We also showed that the first correction term is the same for two point correlation function and  $\sigma^2$ , indeed it is the same for all descriptors of the second moment for which the effective window function goes to unity at small  $k$ .

As an application of our method, we discussed the correction to mass function and multiplicity function using the Press-Schechter as well as the Sheth-Tormen approach. We explicitly wrote down the correction term due to finite box size in each case. We also gave approximate expressions for the correction term and showed that the approximation is very good in case of mass function. We showed that the mass function is always under estimated in simulations due to finite box-size corrections. Multiplicity function, and hence also the number density of haloes of a given mass are underestimated at  $M > M_{nl}$ . At smaller mass scales, however, the multiplicity function is over estimated and we find more haloes in a simulation than expected in the model. The mass scale at which the cross over from under estimate to over estimate occurs is given by Eqn.(10) for Press-Schechter and Eqn.(14) for Sheth-Tormen mass function.

The over estimate at small scales is related to the under estimate of mass in haloes at large scales. If the full power spectrum had been taken into account, the smaller haloes would have merged to form more massive haloes. In absence of large scale modes, the

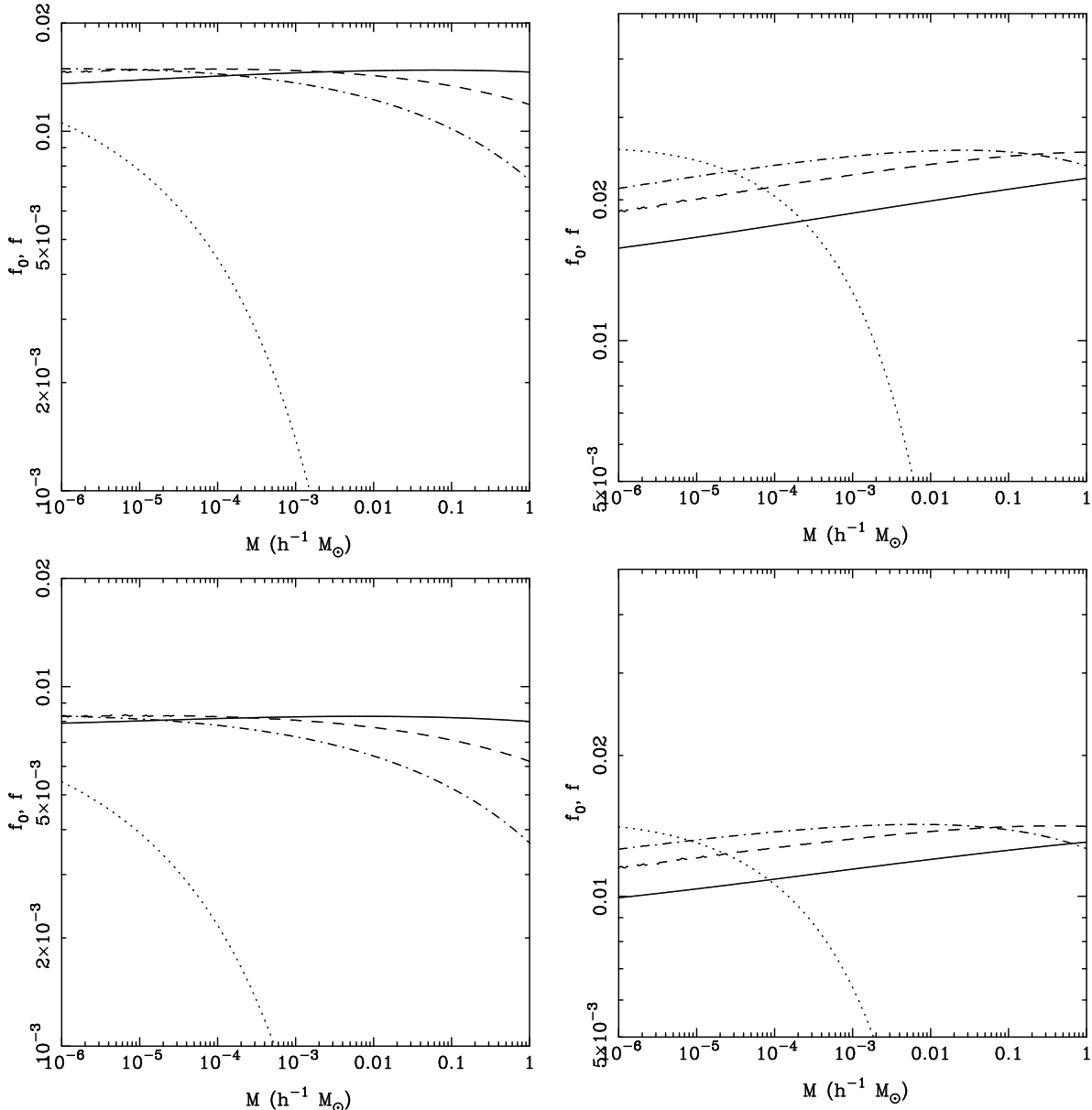


**Figure 5.** The multiplicity function expected in the  $\Lambda$ CDM model (see text for details). The top row is for Press-Schechter mass function and the lower row is for Sheth-Tormen mass function. The left column is for  $z = 20$  and the right column is for  $z = 15$ . The expected multiplicity function is plotted as a function of mass, shown in each panel by a solid curve. Other curves correspond to multiplicity for a finite simulation box:  $L_{\text{box}} = 5h^{-1}\text{kpc}$  (dotted curve),  $L_{\text{box}} = 20h^{-1}\text{kpc}$  (dot-dashed curve) and  $L_{\text{box}} = 100h^{-1}\text{kpc}$  (dashed curve). These correspond to  $C_1/\sigma_0^2 \simeq 0.6, 0.3$  and  $0.19$ , respectively.

formation of massive haloes is slowed down and a larger number of low mass haloes survive.

We find that the over estimate in multiplicity function is large whenever the ratio  $\sigma_1^2(r, L_{\text{box}})/\sigma_0^2(r) \sim C_1(L_{\text{box}})/\sigma_0^2(r)$  is large. To illustrate this correlation, we have plotted the multiplicity function  $f_0(M)$  for the  $\Lambda$ CDM model in Figure 5. This has been plotted for redshift  $z = 20$  and  $z = 15$ . We have also plotted  $f(M, L_{\text{box}})$  here, with  $L_{\text{box}} = 5h^{-1}\text{kpc}$  (dotted curve),  $L_{\text{box}} = 20h^{-1}\text{kpc}$  (dot-dashed curve) and  $L_{\text{box}} = 100h^{-1}\text{kpc}$  (dashed curve). These correspond to  $C_1/\sigma_0^2 \simeq 0.6, 0.3$  and  $0.19$ , respectively. The top row is for the Press-Schechter mass function and the lower row is for the Sheth-Tormen mass function. An identical  $x-y$  range has been used to highlight the differences between the two models for mass function as well. It is noteworthy that the

relative error is similar in both the cases even though the multiplicity function itself is different. At  $z = 20$ , the multiplicity function is under estimated by a large amount for  $L_{\text{box}} = 5h^{-1}\text{kpc}$ , even though  $L_{\text{box}}/r_{nl} \simeq 120$  and if we are interested in scales around 1 pc then  $L_{\text{box}}/r \simeq 5000$ . The situation at small masses is better for the other two simulation volumes considered here. For  $z = 15$ , the scale of non-linearity is  $r_{nl} = 1.4h^{-1}\text{kpc}$ , very close to  $L_{\text{box}} = 5h^{-1}\text{kpc}$  and hence we do not expect believable results for this box-size. Indeed, the two panels on the right demonstrate the large errors and the absurdly incorrect shape of the multiplicity function. The difference in  $f(M)$  and  $f_0(M)$  at  $10^{-6}M_{\odot}$  is about 25% for  $C_1(L_{\text{box}})/\sigma_0^2 = 0.3$ , in this case  $L_{\text{box}} = 20h^{-1}\text{kpc}$  and  $L_{\text{box}}/r \simeq 2 \times 10^4$ . The error in mass function is a little more than 10% for  $L_{\text{box}} = 100h^{-1}\text{kpc}$  even though  $L_{\text{box}}/r \simeq 10^5$

## 8 Bagla and Prasad

and  $L_{\text{box}}/r_{nl} \simeq 67$ . The multiplicity function plotted here is the global function, and one needs to use the conditional mass functions in order to estimate errors in simulations where a high peak is studied at high resolution. Similar results are obtained for other mass functions that have been suggested as a better fit to simulation data (Jenkins et al. 2001; Warren et al. 2005).

The above discussion demonstrates the perils of using simulations where  $C_1(L_{\text{box}})/\sigma_0^2(r)$  is close to unity. One may argue that these models for mass function have not been tested in this regime where the local slope of the power spectrum is very close to  $-3$ , but the fact that error in amplitude of density perturbations itself is large should be reason enough to worry about applicability of results. Further, the agreement in the magnitude of errors for the several approaches to mass functions also gives us some confidence in results.

Majority of simulations are not affected by such serious errors, as the slope of power spectrum approaches  $-3$  only at very small scales (large wave numbers). However, high resolution simulations of earliest structure formation in the  $\Lambda$ CDM model need to have a very large dynamic range before the results can be believed within 10% of the quoted value. Indeed, our work may have some relevance to the ongoing discussion about the Earth mass haloes (Diemand, Moore, & Stadel 2005; Zhao et al. 2005; Zentner, Koushiappas, & Kazantzidis 2005; Moore et al. 2005; Zhao et al. 2005).

In summary, we note that it is extremely important to understand the sources of errors in N-Body simulations and the magnitude of errors in quantities of physical interest. N-Body simulations are used to make predictions for a number of observational projects and also serve as a test bed for methods. In this era of “precision cosmology”, it will be tragic if simulations prove to be weak link. We would like to note that our results apply equally to all methods of doing cosmological N-Body simulations, save those where techniques like MAP are used to include the effects of scales larger than the simulation volume.

The method for estimating errors due to a finite box-size described in this paper can be used for several physical quantities. In this paper we have used the method to study errors in clustering properties and mass functions. We are studying the effect of finite box size on velocity fields and related quantities, the results will be presented in a later publication.

## ACKNOWLEDGEMENTS

Numerical experiments for this study were carried out at cluster computing facility in the Harish-Chandra Research Institute (<http://cluster.mri.ernet.in>). This research has made use of NASA’s Astrophysics Data System.

## REFERENCES

Bagla J. S., 2005, *CSci*, 88, 1088  
 Bagla J. S., Padmanabhan T., 1994, *MNRAS*, 266, 227  
 Bagla J. S., Padmanabhan T., 1997, *MNRAS*, 286, 1023  
 Bagla J. S., Prasad J., Ray S., 2005, *MNRAS*, 360, 194  
 Bagla J. S., Ray S., 2005, *MNRAS*, 358, 1076  
 Bardeen J. M., Bond J. R., Kaiser N., Szalay A. S., 1986, *ApJ*, 304, 15  
 Barkana R., Loeb A., 2004, *ApJ*, 609, 474  
 Bernardeau F., Colombi S., Gaztañaga E., Scoccimarro R., 2002, *Physics Reports*, 367, 1  
 Bertschinger E., 1998, *ARA&A*, 36, 599  
 Bond J. R., Cole S., Efstathiou G., Kaiser N., 1991, *ApJ*, 379, 440  
 Brainerd T. G., Scherrer R. J., Villumsen J. V., 1993, *ApJ*, 418, 570  
 Cole S., 1997, *MNRAS*, 286, 38  
 Colombi S., Bouchet F. R., Schaeffer R., 1994, *A&A*, 281, 301  
 Couchman H. M. P., Peebles P. J. E., 1998, *ApJ*, 497, 499  
 Davis M., Peebles P. J. E., 1977, *ApJS*, 34, 425  
 Diemand J., Moore B., Stadel J., 2005, *Nature*, 433, 389  
 Gelb J. M., Bertschinger E., 1994a, *ApJ*, 436, 467  
 Gelb J. M., Bertschinger E., 1994b, *ApJ*, 436, 491  
 Gunn J. E., Gott J. R. I., 1972, *ApJ*, 176, 1  
 Gurbatov S. N., Saichev A. I., Shandarin S. F., 1989, *MNRAS*, 236, 385  
 Hamilton A. J. S., Kumar P., Lu E., Matthews A., 1991, *ApJL*, 374, L1  
 Hui L., Bertschinger E., 1996, *ApJ*, 471, 1  
 Jain B., Mo H. J., White S. D. M., 1995, *MNRAS*, 276, L25  
 Jain B., Bertschinger E., 1996, *ApJ*, 456, 43  
 Jain B., Bertschinger E., 1998, *ApJ*, 509, 517  
 Jenkins A., Frenk C. S., White S. D. M., Colberg J. M., Cole S., Evrard A. E., Couchman H. M. P., Yoshida N., 2001, *MNRAS*, 321, 372  
 Kanekar N., 2000, *ApJ*, 531, 17  
 Kauffmann G., Melott A. L., 1992, *ApJ*, 393, 415  
 Little B., Weinberg D. H., Park C., 1991, *MNRAS*, 253, 295  
 Ma C., 1998, *ApJL*, 508, L5  
 Matarrese S., Lucchin F., Moscardini L., Saez D., 1992, *MNRAS*, 259, 437  
 Moore B., Diemand J., Stadel J., Quinn T., 2005, [arXiv:astro-ph/0502213](http://arxiv.org/abs/astro-ph/0502213)  
 Nityananda R., Padmanabhan T., 1994, *MNRAS*, 271, 976  
 Padmanabhan T., 1996, *MNRAS*, 278, L29  
 Padmanabhan T., 2002, *Theoretical Astrophysics*, Volume III: Galaxies and Cosmology. Cambridge University Press.  
 Padmanabhan T., Cen R., Ostriker J. P., Summers F. J., 1996, *ApJ*, 466, 604  
 Peacock J. A., 1999, *Cosmological physics*. Cambridge University Press.  
 Peacock J. A., Dodds S. J., 1994, *MNRAS*, 267, 1020  
 Peacock J. A., Dodds S. J., 1996, *MNRAS*, 280, L19  
 Peebles P. J. E., 1974, *A&A*, 32, 391  
 Peebles P. J. E., 1980, *The large-scale structure of the universe*. Princeton University Press.  
 Peebles P. J. E., 1985, *ApJ*, 297, 350  
 Power C., Knebe A., 2005, [arXiv:astro-ph/0512281](http://arxiv.org/abs/astro-ph/0512281)  
 Press W. H., Schechter P., 1974, *ApJ*, 187, 425  
 Sahni V., Coles P., 1995, *Physics Reports*, 262, 1  
 Sheth R. K., Tormen G., 1999, *MNRAS*, 308, 119  
 Sheth R. K., Mo H. J., Tormen G., 2001, *MNRAS*, 323, 1  
 Sirko E., 2005, *ApJ*, 634, 728  
 Smith R. E., Peacock J. A., Jenkins A., White S. D. M., Frenk C. S., Pearce F. R., Thomas P. A., Efstathiou G., Couchman H. M. P., 2003, *MNRAS*, 341, 1311  
 Tormen G., Bertschinger E., 1996, *ApJ*, 472, 14  
 Warren M. S., Abazajian K., Holz D. E., Teodoro L., 2005, [arXiv:astro-ph/0506395](http://arxiv.org/abs/astro-ph/0506395)  
 Zel’dovich Y. B., 1970, *A&A*, 5, 84  
 Zentner A. R., Koushiappas S. M., Kazantzidis S., 2005, [arXiv:astro-ph/0502118](http://arxiv.org/abs/astro-ph/0502118)  
 Zhao H., Taylor J. E., Silk J., Hooper D., 2005, [arXiv:astro-ph/0502049](http://arxiv.org/abs/astro-ph/0502049)

Zhao H., Taylor J. E., Silk J., Hooper D., 2005, arXiv:astro-ph/0508215